Polymer 51 (2010) 6132–6139

Contents lists available at ScienceDirect

Polymer

journal homepage: www.elsevier.com/locate/polymer

Mechanically reinforced biodegradable nanocomposites. A facile synthesis based on PEGylated silica nanoparticles

N. Moussaif [a,*], S. Irusta [b,c], C. Yagüe [b], M. Arruebo [b], J.G. Meier [a], C. Crespo [a], M.A. Jimenez [a], J. Santamaría [b,c]

[a] Technological Institute of Aragon (ITA), María de Luna, 8 (Pol. Actur), 50018 Zaragoza, Spain
[b] Aragon Institute of Nanoscience (INA), Mariano Esquillor s/n, University of Zaragoza, 50018 Zaragoza, Spain
[c] Networking Research Center on Bioengineering, Biomaterials and Nanomedicine, CIBER-BBN, Spain

ARTICLE INFO

Article history:
Received 22 June 2010
Received in revised form
19 October 2010
Accepted 22 October 2010
Available online 30 October 2010

Keywords:
Biopolymers
Polycaprolactone
Nanocomposite

ABSTRACT

Biodegradable nanocomposites consisting of poly(ε-caprolactone) (PCL) reinforced by PEGylated silica (polyethylene-glycol/SiO_2) nanoparticles were prepared by a melt-extrusion process. The PEGylated silica nanoparticles were prepared in a facile, one-pot synthesis process. Transmission electron microscopy (TEM) observations of the PEGylated silica nanoparticles inside the PCL matrix indicated that a homogeneous dispersion had been achieved. As a result, the storage modulus (E') in the rubbery plateau increased significantly with the filler contents at all temperatures studied, at values approximately 45% higher than the neat PCL, at a loading level of only 4 wt.%. In comparison, in the absence of polyethylene-glycol (PEG) the silica nanoparticles formed aggregates inside the PCL matrix, and the reinforcement was negligible. The results from X-ray photoelectron spectroscopy (XPS) and infrared spectroscopy (FTIR) analyses identified the location of the PEG at the PCL/silica interface.

1. Introduction

Polycaprolactone (PCL) is a linear, hydrophobic and partially crystalline aliphatic polyester. It is often considered as a *green* polymer on account of its biocompatibility and biodegradability by microorganisms [1,2]. Its physical properties and commercial availability make it attractive as a substitute for non-biodegradable polymers in commodity applications such as biodegradable packaging [3], but also as a plastic in a variety of specialized uses, including medical devices, controlled drug release systems, and agricultural applications [4–6]. However, a wider use of PCL is hampered by its low melting temperature (Tm ~ 65 °C), low elastic modulus and low abrasion. Additionally, its poor barrier properties to water and gases create a further obstacle to its use as biodegradable packaging material [7]. In summary, there is considerable interest in the improvement of the mechanical and barrier properties of PCL, and the development of PCL nanocomposites constitutes one of the most attractive possibilities.

In the last two decades considerable research interest in polymer nanocomposites has developed, driven by the possibility of developing polymeric materials with improved/tuned properties through the incorporation of these nanoscale materials into a polymer matrix. Commonly observed enhancements concern mechanical properties, thermal stability, gas barrier properties, electric properties, and even biodegradation rates [7]. Low additions (typically less than 5 wt.%) of nanostructured materials (e.g. layered silicates) to polymers often yield remarkable improvements in specific properties (e.g. mechanical resistance, barrier effectiveness) of the polymer [3,8–12]. Attaining comparable improvements with conventional fillers would require loadings of 30–50 wt.%.

Because of their small size, nanomaterials have large external areas. Uniform dispersion of these nanofillers in a polymer produces an ultra-large interfacial area density (m^2 of interfacial area per unit volume of composite) between the nanomaterial and the host polymer. This interfacial region is generally responsible for the specific characteristics of polymer-based nanostructured materials when compared to traditional composites [13]. However, a good dispersion is not easy to achieve: the different nature of the nanofiller (inorganic) with respect to the polymer matrix (organic) is responsible for a strong tendency to form aggregates. This runs contrary to the fact that an excellent dispersion is needed, since the performance of nanomaterials is related to the degree of homogeneity achieved in the dispersion of the nanofiller. As a solution, functionalization of the nanomaterials to facilitate dispersion in the

* Corresponding author. Tel.: +34 976 010 021; fax: +34 976 011 888.
E-mail address: nmoussaif@ita.es (N. Moussaif).

0032-3861/$ – see front matter © 2010 Elsevier Ltd. All rights reserved.
doi:10.1016/j.polymer.2010.10.042

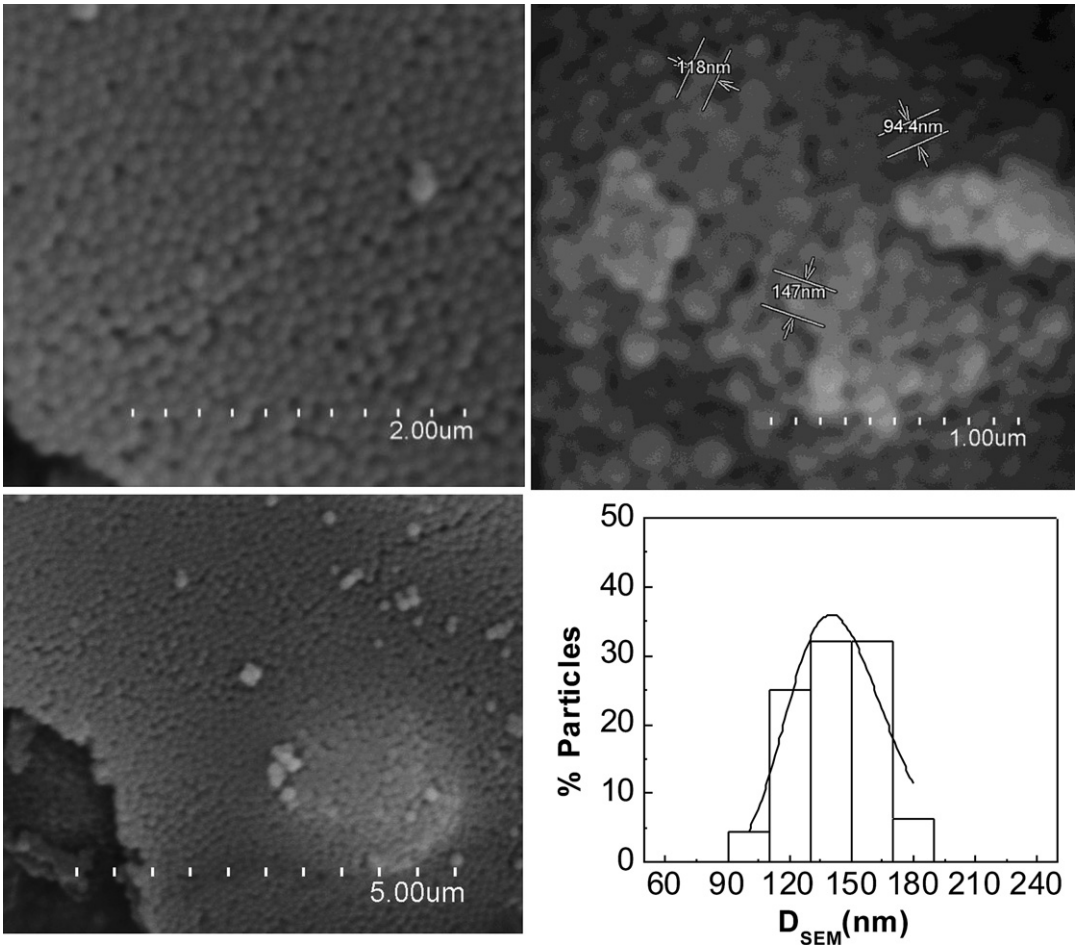

Fig. 1. Scanning electron photographs of the PEGylated nanoparticles. Particle-size distribution.

polymer matrix is often used. A good example of this approach for silica nanoparticles is the work of Shin et al. [14] who treated silica nanoparticles with triethoxyvinylsilane (VTES) as a coupling agent to introduce vinyl groups. VTES functionalized silica nanoparticles were then grafted with poly(ethylene glycol) (PEG) via UV-photopolymerization in order to increase the interactions between the polymeric matrix and the silica nanoparticles.

Many attempts have been made to formulate nanocomposites with PCL in order to improve its mechanical and thermal resistance properties. Perhaps the most common group of nanofillers are the organophilic modified layered silicates [3,15–20]. PCL nanocomposites with modified and unmodified montmorillonite or multi-walled carbon nanotubes [21–23] have been reported in the literature, prepared either by *in situ* polymerization, melt mixing or by the solvent-casting method. On the other hand, silica is also a commonly used nanofiller on account of its ease of preparation and functionalization. In a study by Chen et al., nanocomposites of PCL castable polyurethane elastomer with nanosilica particles having different surface properties were prepared via *in situ* polymerization [24]. The surface treatment by the different coupling agents influenced the dispersibility of the SiO_2 in the PCL CPUE (castable polyurethane elastomer). Thus, agglomerates with more than 1 μm diameter were observed when untreated nanosilica was used, while silica nanoparticles pretreated with γ-glycidochloropropyl methyl trimethoxy silane were homogenously dispersed in the PCL CPUE. Avella et al. also prepared nanocomposites based on a moderate molecular weight PCL and silica nanoparticles that had previously been functionalized by grafting with aminopropyltriethoxysilane (APTES) [25]. The PCL nanocomposites were then prepared by extrusion, giving a fine distribution of the nanoparticles in the matrix together with a good interfacial adhesion between the two phases. It has also been proposed that the biodegradability of PCL can be enhanced by copolymerizing or blending it with other hydrophilic polymers such as PEG. This water-soluble and non-toxic polymer can be used to increase the rate of biodegradation in PCL/PEG microcapsules containing fragrant oil adsorbed on SiO_2 [26]. PEG is a polar homopolymer that, in spite of being hydrophilic, is compatible with the PCL matrix [27]. It has been used in previous works to create a hydrophilic organic shell around silica nanoparticles for drug delivery applications [28] and its ability to prevent agglomeration of silica nanoparticles has also been demonstrated [28]. In the present work, in order to obtain a nanocomposite with good biodegradable properties and at the same time with enhanced mechanical and physical properties we have used PEG-functionalized (termed PEGylated) silica nanoparticles as fillers. It is important to point out that, unlike previous works, the synthesis and functionalization of the nanofiller here have been performed in a single step, by including PEG in the synthesis medium of the silica nanoparticles. This not only simplifies the synthesis process, but is also thought to contribute to a better adhesion of PEG to the nanofiller. Once the PEGylated nanoparticles were prepared, the composite was obtained through conventional melt-processing techniques (extrusion) in an environmentally friendly way that avoids the use of solvents. A battery of techniques has been used to characterize both PEGylated silica nanoparticles and the

nanocomposites obtained. Special attention has been paid to the influence of PEG on the mechanical properties of the composites, and to confirm the location of the PEG at the PCL/silica interface.

2. Experimental

2.1. Materials, synthesis and preparation

The synthesis of PEGylated silica particles was carried out following the procedure described by Xu et al. [29]. Briefly, 2 g of poly(ethylene glycol) with a molecular weight of 3000 g/mol was dissolved in 6 ml ammonium hydroxide solution (30 wt.% NH_3) and 24 ml methanol in a first step. 0.2 ml of tetramethyl orthosilicate (TMOS) was added dropwise and after stirring for 4 h, the samples were filtered and washed with ethanol. The pellet was re-dispersed in distilled water and freeze-dried using lyophilization to stabilize it for storage and later use. All chemicals were purchased from Sigma–Aldrich and used as-received.

Polycaprolactone (PCL) with a molecular weight around 1,20,000 g/mol was used to prepare nanocomposites with, 2, 3 and 4 wt.% of filler (dry PEGylated SiO_2 nanoparticles) by loading into a twin-screw mini-extruder (DSM-Xplore 15 Microcompounder, Model 2005). An intimate mixture was achieved at 100 °C for 10 min, with a rotation speed of 100 rpm and under nitrogen atmosphere. Both of polymer and nanoparticles were previously dried overnight in a vacuum oven at 50 °C before the extrusion process. In the remainder of this work, samples are named PCL/*x* SiO_2, where *x* is the wt.% of PEGylated particles added to the polymeric matrix. For comparison, a PCL composite filled with 3 wt.% of non-modified silica (named PCL/SiO_2) has also been prepared using the same experimental conditions except for the presence of PEG.

2.2. Characterization

BET surface areas, N_2 adsorption/desorption isotherms, and pore-size distributions of the silica nanoparticles were obtained using a Micromeritics ASAP 2020 V1 device at 77 K. The particle-size distribution of the dispersed materials in aqueous dispersions was obtained by photon correlation spectroscopy (PCS) (Malvern Zetasizer 3000 HS). Thermogravimetric analyses (TGA) were carried out in a TGA/SDTA851 system (Mettler Toledo) under air at a heating rate of 10 °C/min. Fourier transform infrared (FTIR) spectroscopy of the composites was performed with a Bruker Vertex 70 FTIR spectrometer equipped with a DTGS detector and a Golden Gate diamond ATR accessory. Spectra were recorded by averaging 40 scans in the 4000–600 cm^{-1} wavenumber range at a resolution of 4 cm^{-1}. Data evaluation was carried out by using the OPUS software from Bruker Optics, Inc. X-ray photoelectron analysis (XPS) was performed with an Axis Ultra DLD (Kratos Tech.). The spectra were excited by the monochromatized AlKα source (1486.6 eV) run at 15 kV and 10 mA. For the individual peak regions, a pass energy of 20 eV was used. Each survey spectrum was measured at 160 eV pass energy. Analyses of the peaks were performed with CasaXPS software, using a weighted sum of Lorentzian and Gaussian component curves after background subtraction. The binding energies were referenced to the internal C 1s (284.9 eV) standard. The morphology and size distribution of PEGylated nanoparticles were examined by scanning electron microscopy, SEM (JEOL JSM 6460 LV and Hitachi S2300). Statistical size-distribution histograms for the resulting nanoparticles were produced from SEM images using Image J software (sample size = 30). Ultra-thin sections of the nanocomposite materials with thicknesses of approximately 60–80 nm were cut under cryogenic conditions with a Leica Ultramicrotome equipped with a diamond knife. Transmission electron microscopy (TEM) was carried out in a JEOL 2000 FXII apparatus using an acceleration voltage of 200 kV. Due to the high electron density difference between the silica and the polymer, staining of the PCL nanocomposite samples was not needed.

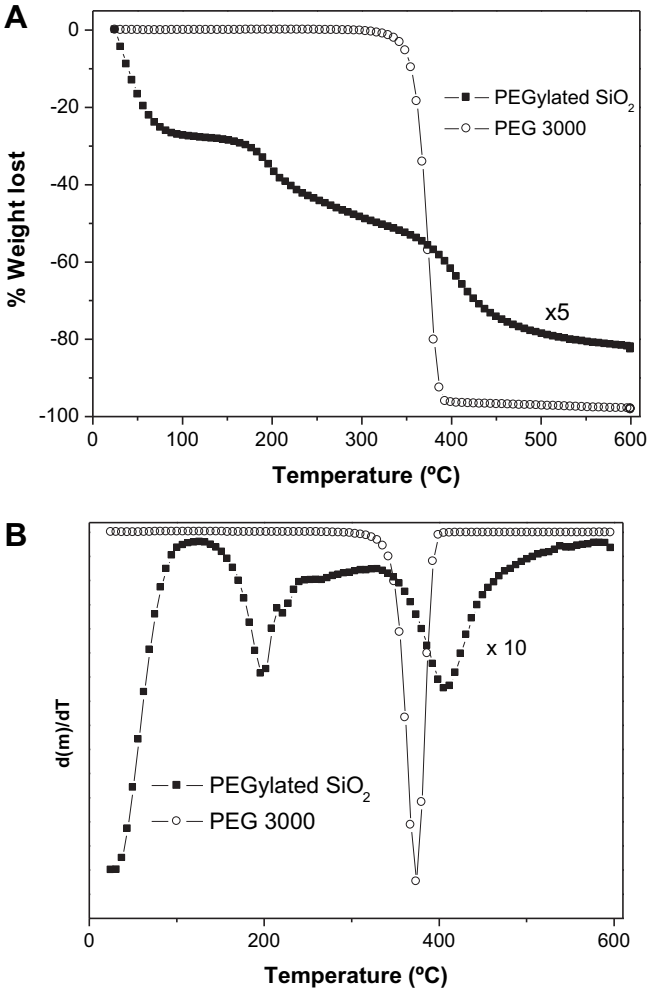

Fig. 2. TGA under air results for PEG and for PEGylated silica samples. A) mass loss, B) DTGA.

Thermal analysis of the samples was preformed using a DSC822 Mettler Toledo differential scanning calorimeter. All the experiments were carried out under nitrogen atmosphere as follows: the samples were heated up to 100 °C at a rate of 10 °C/min and held for 5 min to remove any residual crystals, which could act as seeds in the following crystallization. The samples were then cooled to room temperature and heated to 100 °C at a rate of 10 °C/min. The melting enthalpy of this second heating run was, after normalization to the PCL mass, converted to a PCL crystallinity using a reference ΔH_f value of 136.1 J/g for the melting of 100% of crystalline PCL [30].

Dynamic mechanical properties of the base PCL and of the PCL nanocomposites with different loadings were measured with a DMA + 450 Metravib, using a bar specimen of 25 mm length, 7 mm width and 2 mm thickness in the tension jaws for bar mode at an oscillation frequency of 1 Hz at temperatures ranging from 30 to 60 °C and with a heating rate of 2 °C/min.

3. Results and discussion

According to the SEM images (Fig. 1), the synthesized PEGylated particles are uniform in size (with a distribution centered at 140 nm).

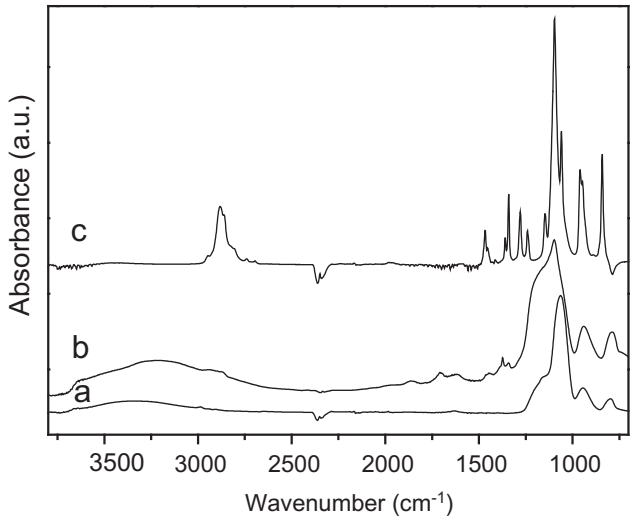

Fig. 3. FTIR spectra for the PEG and the PEGylated silica nanoparticles. (a) SiO_2 nanoparticles, (b) SiO_2/PEG, (c) PEG.

An aqueous suspension of the PEGylated silica nanoparticles at a neutral pH showed a particle-size distribution centered at 147.4 nm, which is coincident with the SEM observations, indicating that the particles remain dispersed in water without agglomeration. On the other hand, in aqueous suspension the non-modified SiO_2 forms agglomerates of a size that cannot be measured by PCS (larger than 2 μm). This is in agreement with previous reports [28] on the role of PEG in preventing the agglomeration of silica nanoparticles.

The nanoparticles showed a modest BET surface area of 136.3 ± 1.5 m^2/g and a type II isotherm characteristic of non-porous materials with a small hysteresis between the adsorption and desorption branches, indicating a limited mesoporosity. The sample did not show any microporosity (*t-plot* results). The TGA and DTGA profiles for the PEGylated SiO_2 are shown in Fig. 2, where the PEG curve has also been added for comparison. The first weight lost at low temperatures for the PEGylated sample (Fig. 2B) is related to the desorption of ethanol or water physically adsorbed and/or H-bonded to the silica matrix [29]. The second peak of the DTGA profile starts at around 120 °C with the maximum at 195 °C, and the third weight loss is in the range 300–550 °C with a maximum at 410 °C. Grandi et al. [31] assigned a peak in the range 250–350 °C to the evolution of chemically bound water, but they did not rule out

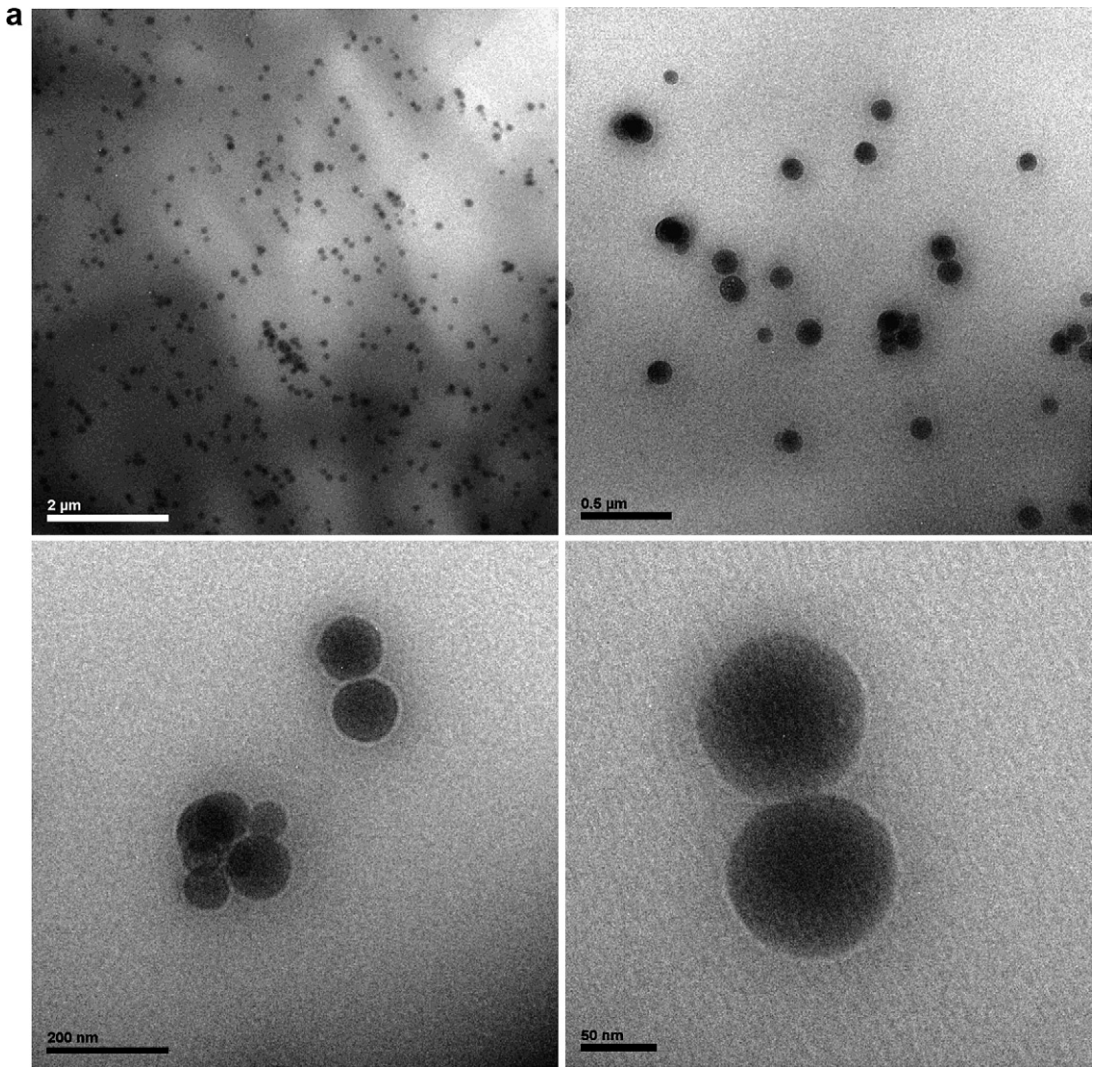

Fig. 4. a) TEM micrographs of PCL with 3 wt.% of PEGylated silica nanoparticles (SiO_2-PEG) with different magnifications. b) TEM micrographs of PCL with 3 wt.% of non-modified silica nanoparticles (SiO_2) with different magnifications.

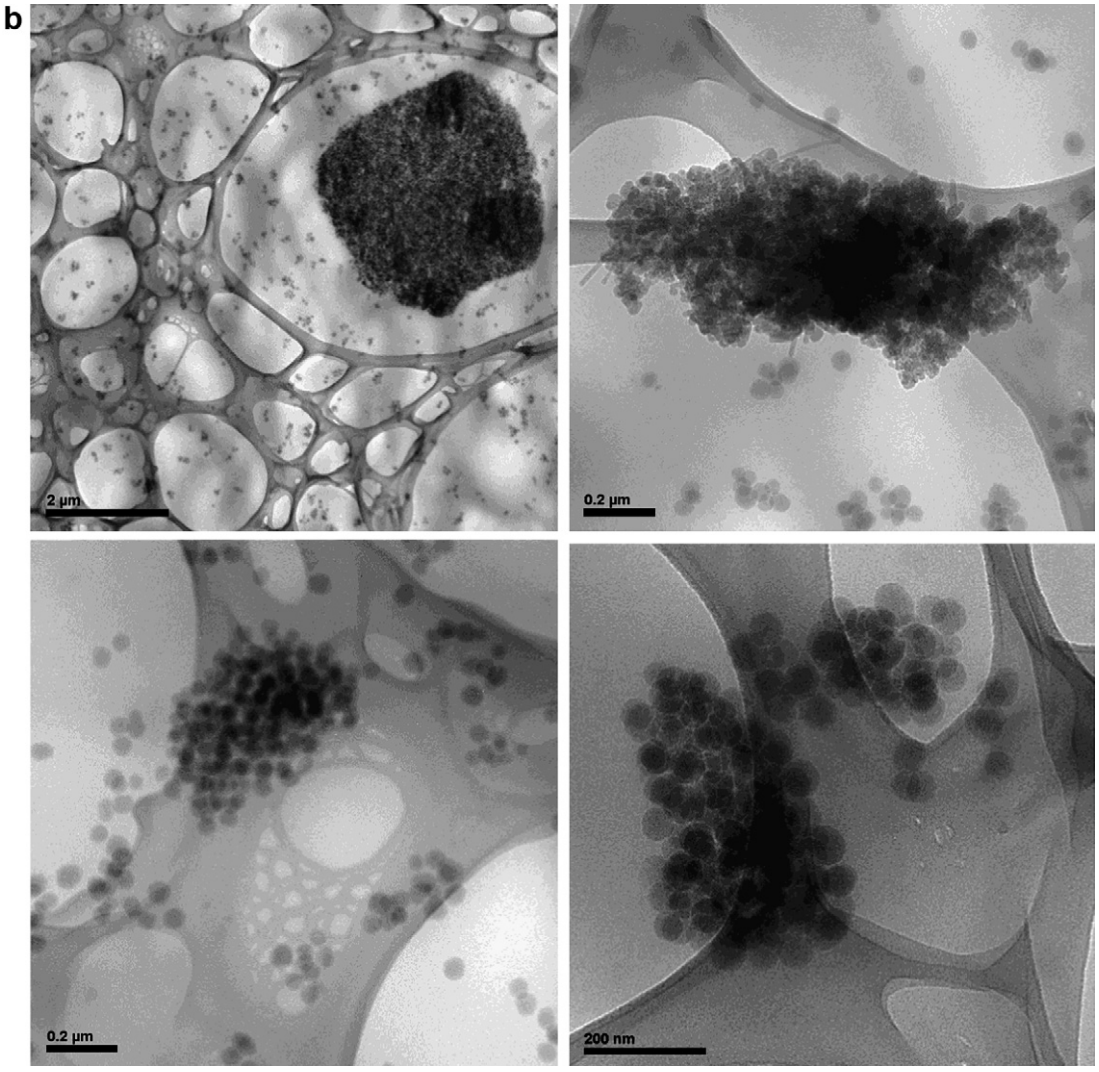

Fig. 4. (*continued*).

the evolution of some molecules of ethanol strongly H-bonded to the silica-PEG matrix. The last peak is due to the embedded PEG decomposition in gaseous by-products, such as CO_x [31]. The PEG-SiO_2 sample is thermally stable up to 410 °C. For comparison, the non-attached PEG is limited to 372 °C and this improvement clearly suggests that the organic moieties are bonded to the SiO_2 matrix [31]. Taking into account the last weight loss, the PEG content in the hybrid nanoparticles was calculated as 5.8 wt.%.

FTIR spectra of SiO_2 and PEGylated silica particles are shown in Fig. 3, where the PEG spectrum was added for comparison. Both particle spectra show the contribution of the hydroxyl groups with absorption ranging from 3700 to 2600 cm^{-1}. These groups would be related to adsorbed water, and this band is more important for the PEGylated silica since these particles become more hydrophilic due to the PEG molecules [32]. Peaks at 1065 and 800 cm^{-1} in the SiO_2 spectrum are characteristic of the asymmetric and symmetric Si—O—Si stretching vibrations, respectively [33]. The band at 947 cm^{-1} is attributed to (Si—OH) [34]. FTIR results for the PEGylated nanoparticles showed bands in the 2970–2800 cm^{-1} region characteristic of the CH_2 symmetric and anti-symmetric stretching modes that clearly indicate the presence of PEG on the surface of the silica nanoparticles. Peaks at 1372 and 1342 cm^{-1} would be related to the CH_2-wagging bands of PEG [35]. Even though contributions associated with PEG in the range 1300–700 cm^{-1} overlap with Si—O—Si asymmetric stretching bands [36], there is a clear shift of the maximum of this peak from 1065 to 1097 cm^{-1}. This change could be related to the presence of the asymmetric Si—O—C stretching mode [37], or could be related to the PEG bands associated to the C—O and C—C stretching modes. Since no change was observed at around 833 cm^{-1} where the symmetric Si—O—C stretching mode occurs, the change can be attributed to the effect of PEG.

3.1. Nanocomposites morphology

Transmission electron microscopy (TEM) was used to examine the morphology of the nanocomposites based on PCL and PEGylated/non-modified (non PEGylated) silica nanoparticles. Fig. 4a and b shows TEM micrographs of PCL containing 3 wt.% of PEGylated silica and non-modified silica, respectively, where the dark domains corresponding to the silica particles in the polymer matrix can be observed. The same experimental conditions for dispersion were used in both cases. A nanoscale dispersion of individual PEGylated silica particles, with uniform size, is observed (Fig. 4a), while the non-modified silica nanoparticles appear highly agglomerated in the matrix (Fig. 4b). These observations point to the beneficial effect of PEG as an interfacial compatibilizer, capable

of reducing the interfacial tension between the silica particles and the PCL and giving rise to a homogeneous distribution of the nanofillers. Similar results were obtained by Avella et al. [25]. The nanocomposite with aminopropyltriethoxysilane/SiO_2 showed a good distribution of the nanoparticles in the matrix together with a good interfacial adhesion between the two phases, while large aggregates were present in the case of material filled with non-modified silica.

For further characterization of the interfacial activity of PEG at the silica/PCL interface, the interactions between the PEG and the silica and between the PEG and the PCL have been studied by XPS and FTIR. The XPS analyses performed for SiO_2, PEGylated nanoparticles and PCL nanocomposites are summarized in Table 1. The binding energy (BE) of the Si 2p peak measured in the bare particles is 103.5 eV, typical for silicon atoms coordinated with oxide anions in SiO_2. In the PEGylated sample, the Si 2p BE shifted to lower values (101.8 eV) indicating a different electronic environment for the Si related to the aforementioned interaction between the silica particles and the organic compound [38]. The Si 2p BE in the nanocomposite materials (Table 1) is also similar to that in the PEGylated nanoparticles, suggesting the location of the PEG at the interface between PCL and silica. On the other hand, in the composite with non-functionalized particles the Si 2p BE is again 103.8 eV, showing the lack of interaction between the polymer and the inorganic particles.

FTIR spectra of PCL and the SiO_2/PCL nanocomposites are shown in Fig. 5(A and B). The increase of the shoulder at 1096 cm^{-1} observed in the spectrum of the nanocomposites would be related to the silica vibrations (Fig. 5A). Fig. 5B shows the band at 1721 cm^{-1} characteristic of the carbonyl stretching of the PCL. Even though it remains almost at the same wavenumber for the nanocomposite containing 2 wt.% of PEGylated SiO_2 and for the composite with non-functionalized silica, it shifts to a lower wavenumber when a higher PEGylated particle content (4 wt.%) is introduced. According to Lin and Lu [39] the shift of the carbonyl stretching band would be related to the interaction between PCL and PEG. An interaction was also observed between PEG and carboxyvinyl polymer, which has the same functional group as PCL [40]. This interaction could be explained by the formation of an interpenetrating network structure as a result of hydrogen bonds between the C—OH group (H donator) of PEG and the carboxylic group (H-acceptor) of the repeated units of the caprolactone, indicating again the location of the PEG at the PCL/silica interface, in good agreement with the XPS results.

3.2. Crystallinity (DSC)

Crystallinity could affect the mechanical properties of the composite material since a higher fraction of crystals produces an increment in the strength and modulus of the material [30]. Table 2 shows the degree of crystallinity and the melting temperature of pure PCL and PCL nanocomposite containing 3 wt.% of the PEGylated silica. It can be seen that the incorporation of PEGylated silica does not significantly affect the melting behavior of the PCL. The degree of crystallinity remained, indeed, unchanged for both of PCL and PCL nanocomposite.

Table 1
XPS results for particles and composite materials.

Sample	Binding energy (eV)		
	C 1s	O 1s	Si 2p
SiO_2	284.9	532.7	103.5
PEGylated SiO_2	284.9	531.1	101.8
PCL/2 wt.% SiO_2-PEG	284.9	532.2	102.1
PCL/3 wt.% SiO_2-PEG	284.9	532.0	101.9
PCL/4 wt.% SiO_2-PEG	284.9	532.0	102.0
PCL/3 wt.% SiO_2	284.9	532.0	103.8

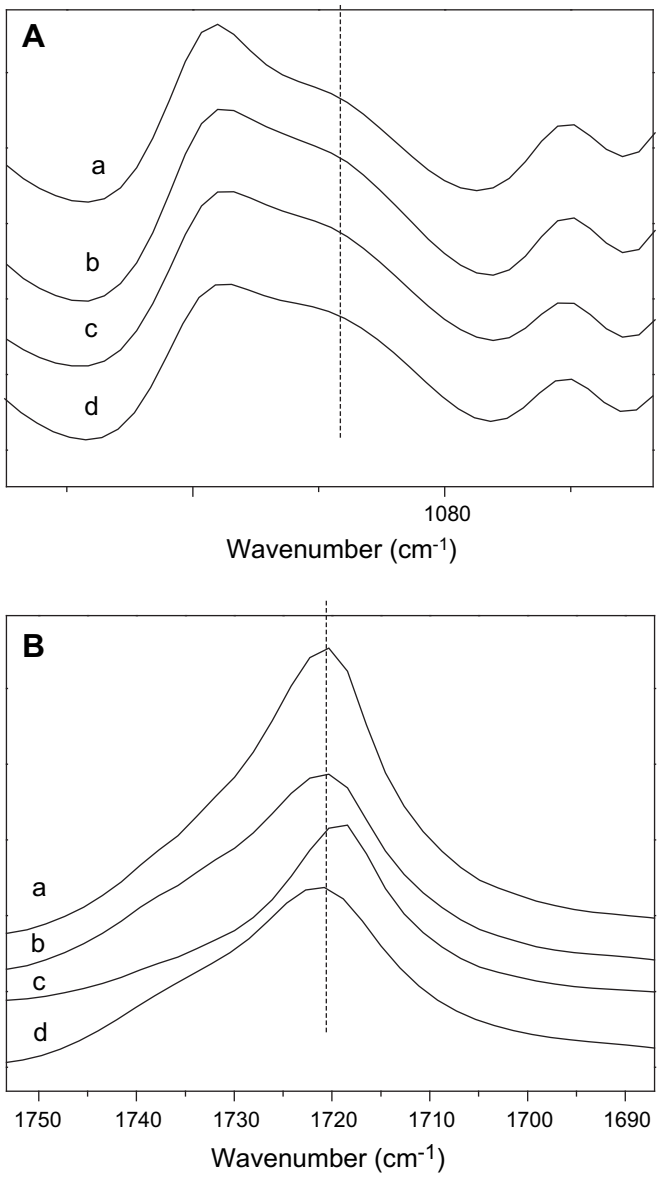

Fig. 5. FTIR spectra of a) PCL, b) PCL/2 wt.% SiO_2-PEG, c) PCL/4 wt.% SiO_2-PEG, d) PCL/3 wt.% SiO_2.

3.3. Dynamic mechanical analysis (DMA)

The investigation of the mechanical properties of the polymer composites is another interesting tool for examining the strength of the interaction between the PCL matrix and the reinforcing particles (SiO_2). Good interfacial interactions mean a good transfer of an external load from the matrix to the particles, resulting in the improvement of the mechanical performance of the composite material [25]. PCL, PCL composite containing 3 wt.% of non-modified silica and PCL nanocomposites with different PEGylated-silica loading have been characterized by dynamic mechanical analysis. The temperature dependence of the elastic modulus (E')

Table 2
DSC data of PCL (nano)composites obtained from 2nd run (heating).

Sample	Tm (°C)	ΔH_f (J/g)	χ_c (%)
PCL	66.1	57.6	43.6
PCL/3 wt.% SiO_2-PEG	68.6	55.9	43.6

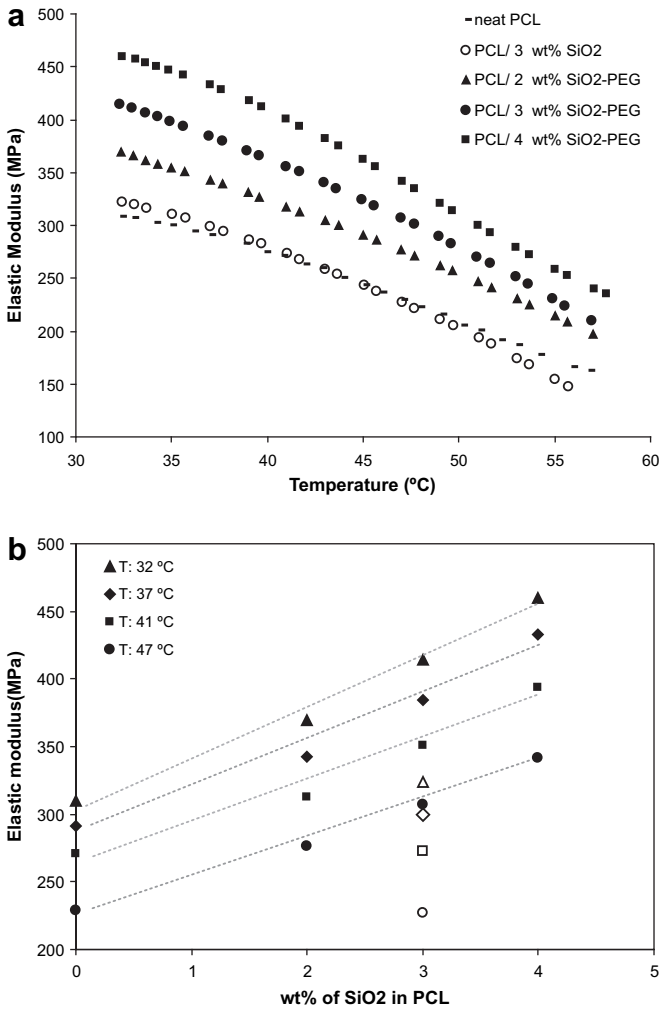

Fig. 6. a) Dependence of the elastic modulus on the temperature for different amounts of SiO_2-PEG and SiO_2 (open symbol) in PCL nanocomposites. b) Dependence of the elastic modulus on the amount of SiO_2-PEG (filled symbol) and SiO_2 (open symbol) in PCL nanocomposites for different temperatures.

for these samples is shown in Fig. 6a, while the dependence of the elastic modulus on the amount of SiO_2-PEG in the PCL nanocomposites at 32, 37, 41 and 47 °C is represented in Fig. 6b and summarized in Table 3. The PCL containing 3 wt.% of non-modified silica behaves almost the same as the neat PCL, which would be a consequence of the aggregated microstructure that was observed by TEM (Fig. 4b). However, the dynamic-mechanical results of the PCL nanocomposites based on PEGylated silica exhibit a clear increase of E' as the weight percentage of the nanofiller increases (see Fig. 6a). In fact, at 32, 37, 41 and 47 °C, the storage modulus (E')

Table 3
Dependence of the elastic modulus on the amount of SiO_2-PEG in PCL nanocomposites for different temperatures. ΔE is % of the increase of the modulus as compared to the neat PCL.

Sample	32 °C		37 °C		41 °C		47 °C	
	E' (MPa)	$\Delta E'$ (%)	E' (MPa)	$\Delta E'$ (%)	E' (MPa)	$\Delta E'$ (%)	E' (MPa)	$\Delta E'$ (%)
PCL	310	0	291	0	271	0	229	0
PCL/2 wt.% SiO_2-PEG	370	19.4	343	17.9	313.1	15.5	276.7	20.8
PCL/3 wt.% SiO_2-PEG	414	33.5	384.8	32.2	350.7	29.4	307.1	34.1
PCL/4 wt.% SiO_2-PEG	460	48.5	433.1	48.8	394.1	45.5	341.7	49.2

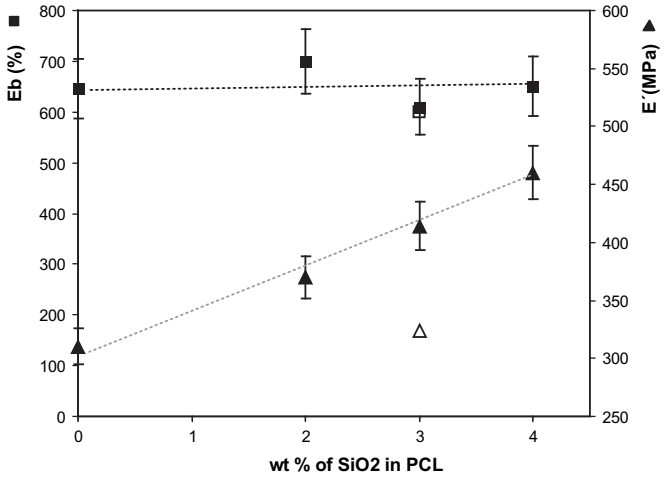

Fig. 7. Dependence of elastic modulus (E' at 32 °C) and elongation at break (Eb at room temperature) on the amount of SiO_2-PEG (filled symbol) and SiO_2 (open symbol) for PCL nanocomposites.

of the nanocomposites containing 4 wt.% of PEGylated silica are approximately 48, 49, 45 and 49% higher compared to the PCL matrix, respectively (Table 3). Fig. 7 shows the dependence of E' (at 32 °C) and the maximum elongation at break (at room temperature) with the silica content in the PCL nanocomposites. The maximum elongations at break of all of these nanocomposites are similar to that of the neat PCL and remain independent of the silica loading in these silica-content ranges. PCL is a ductile polymer able to sustain substantial deformation. Nanocomposites with PEGylated nanoparticles will remain ductile with an elongation at break around 650%.

PCL nanocomposites with PEGylated SiO_2 showed high stiffness at least up to a silica loading of 4 wt.% due to the high dispersion of the filler and the good nanoparticle–polymer interaction. The composites indeed maintain a good ductility in the loading range studied.

In summary, since as already discussed the mechanical performance of polymer composites is generally associated with the strength of the interaction between the matrix and the reinforcing, it seems clear that the action of PEG as compatibilizing agent improves the dispersion of the nanoparticles and the interfacial adhesion to the matrix, with a strong effect on the properties of the composite and its mechanical performance. More specifically, the increase in E' with temperature with respect to that of the PCL matrix can be attributed to a higher reinforcement effect of the fillers at the nanoscale due to the restricted movement of the polymer chains above the Tg [41].

4. Conclusions

PCL/PEG/SiO_2 nanocomposite materials were successfully prepared by melt-extrusion, using PEGylated silica nanoparticles prepared in a facile, one-pot synthesis. The role of PEG as an interfacial agent was investigated with respect to the morphological and dynamic mechanical properties of these nanocomposite materials. A homogeneous distribution of the individual silica particles was obtained when the PEGylated silica was used, while the same silica nanoparticles aggregated severely when they were not functionalized. The XPS analysis studied in correlation with the FTIR data provided evidence for locating PEG at the silica/PCL interface. No changes have been observed in the crystallinity of PCL when the PEGylated silica was added. From the dynamic mechanical measurements, a clear increase in the elastic moduli of the

nanocomposites with increasing PEGylated silica content was observed at all the temperatures studied. This enhancement of the storage modulus in the rubbery plateau for PCL nanocomposites compared to the neat PCL matrix occurs for moderate filler contents (under 4 wt.%), and is a result of the high dispersion of the filler and the good nanoparticle–polymer interaction. In addition, the elongation at break of these nanocomposites at room temperature remained similar to that of the neat PCL over all the loading range.

Acknowledgements

The authors are grateful to the "Ministerio de Ciencia & Innovación" for the financial support for this research (XDEX-60900-2008-17). One of the authors, N.M. is indebted to the "Fundación Agencia Aragonesa para la Investigación y el Desarrollo (ARAID)" for supporting this research. M.A. would like to acknowledge support from the 2006 "Ramón y Cajal" program (order ECI/158/2005).

References

[1] Hung SJ, Edelman PG. In: Scott G, Gilead D, editors. Degradable polymers: principles and applications. London: Chapman & Hall; 1995 [chapter 2].
[2] Kesel CD, Wauven CV, David C. Polym Degrad Stab 1997;55:107.
[3] Messersmith PB, Gianellis EP. J Polym Sci A Polym Chem 1995;33:1047.
[4] Dubois P, Jacobs C, Jerome R, Teyssie P. Macromolecules 1991;24:2266.
[5] Potts JE, Jelinek HHG, editors. Aspect degradation and stabilization of polymers: Amsterdam; 1965.
[6] Ma PX. Mater Today 2004;7:30.
[7] Chrissafis K, Antoniadis G, Paraskevopoulos KM, Vassilio A, Bikiaris DN. Composites Sci Tech 2007;67:2165.
[8] Pinnavaia TJ, Beall GW, editors. Polymer-clay nanocomposites. New York: Wiley; 2000.
[9] Giannelis E. Adv Mater 1996;8:290.
[10] Maiti P, Nam PH, Okamoto M, Hasegawa N, Usuki A. Macromolecules 2002;35:2042.
[11] Fischer HR, Gielgens LH, Koster TPM. Acta Polym 1999;50:122.
[12] Moussaif N, Groeninckx G. Polymer 2003;44:7899.
[13] Henglein A. Chem Rev 1989;89(8):1861.
[14] Shin Y, Lee D, Lee K, Ahn K, Kim B. J Ind Eng Chem 2008;14:515.
[15] Usuki A, Kojima Y, Kawasumi M, Okada A, Fukushima Y, Kurauchi T. J Mater Res 1993;8:1179.
[16] Messersmith PB, Giannelis EP. Chem Mater 1993;5:1064.
[17] Lim ST, Hyun YH, Choi HJ, Jhon MS. Chem Mater 2002;14:1839.
[18] Lepoittevin B, Devalckenaere M, Pantoustier N, Alexandre M, Kubies D, Calberg J, et al. Polymer 2002;43:4017.
[19] Homminga DS, Goderis B, Dolbnya I, Reynaers H, Groeninckx G. Polymer 2006;47:1620.
[20] Kiersnowski A, Piglowski J. Eur Polym J 2004;40:1199.
[21] Saeed K, Park S, Lee H, Baek J, Huh W. Polymer 2006;47:8019.
[22] Miltner H, Watzeels N, Block C, Gotzen N, Van Assche G, Borghs K, et al. Eur Polym J 2010;46:984.
[23] Sanchez-Garcia M, Lagaron J, Hoa S. Composites Sci Tech 2010;70:1095.
[24] Chen XD, Zhou NQ, Zhang H. J Phys Conf Ser 2009;188:012025.
[25] Avella M, Bondioli F, Cannillo V, Di Pace E, Errico ME, Ferrari AM, et al. Composites Sci Tech 2006;66:886.
[26] Park SJ, Yang YJ, Lee HB. Colloids Surf B Biointerfaces 2004;38:35.
[27] Cai Q, Bei J, Wang S. Polymer 2002;43:3585.
[28] Yagüe C, Moros M, Grazú V, Arruebo M, Santamaría J. Chem Eng J 2008;137:45.
[29] Xu H, Yan F, Monson EC, Kopelman R. J Biomed Mater Res A 2003;66A:870.
[30] Ludueña L, Alvarez V, Vazquez A. Mater Sci Eng 2007;460:121.
[31] Grandi S, Magistris A, Mustarelli P, Quartarone E, Tomasi C, Meda L. J Non-Cryst Solids 2006;352:273.
[32] Dorati R, Genta I, Tomasi C, Modena T, Colonna C, Pavanetto F, et al. J Microencapsul 2008;25:330.
[33] Muroya M. Colloids Surf A Physicochem Eng Asp 1999;157:147.
[34] Khalil KMS, Makhlouf SA. Appl Surf Sci 2008;254:3767.
[35] Matsura H, Miyazawa T. J Pol Sci 1969;7:1735.
[36] Nishio K, Okubo K, Watanabe Y, Tsuchiya T. J Sol-gel Sci. Tech 2000;19:187.
[37] Chiang C, Ishida H, Koening JL. J. Colloid Interface Sci 1980;74:396.
[38] Zornoza B, Irusta S, Téllez C, Coronas J. Langmuir 2009;25:5903.
[39] Lin WJ, Lu CH. J Memb Sci 2002;198:109.
[40] Ozeki T, Yuasa H, Kanaya Y. J Control Release 1999;58:87.
[41] Sinha RS, Okamoto M. Prog Polym Sci 2003;28:1539.